

**On thermoelectric power conversion from heat re-circulating combustion systems**

F. J. Weinberg

Imperial College, London, SW7 2BY

D. M. Rowe and G. Min

NEDO Laboratory, School of Engineering, Cardiff University, Cardiff, CF24 3TF

and

P. Ronney

University of Southern California, Los Angeles, CA 90089-1453

This paper is intended for

**Colloquium No 14 “New Concepts...MICRO-COMBUSTORS”**

**Corresponding Author:**

Prof. Felix Weinberg

Department of Chemical Engineering and Chemical Technology

Imperial College of Science, Technology and Medicine

Prince Consort Road

London, SW7 2BY

e.mail: f.weinberg@ic.ac.uk

‘Phone 4420 8876 1540

Fax: 4420 7594 5604

Word count: 3750

Diags. equivalent: 1600

5350

# **On thermoelectric power conversion from heat re-circulating combustion systems**

F. J. Weinberg  
Imperial College, London, SW7 2BY

D. M. Rowe and G. Min  
NEDO Laboratory, School of Engineering, Cardiff University, Cardiff, CF24 3TF

P. Ronney  
University of Southern California, Los Angeles, CA 90089-1453

## **Abstract**

The thermodynamic theory governing the absolute maximum efficiency of energy conversion by thermoelectric devices that operate as part of the heat recycle in regenerative burners, is examined. Comparison with series of elementary Carnot cycles helps to address the question of whether higher system efficiencies are realisable by rejecting the unconverted heat to the cold surroundings or to the incoming reactants as part of the recycle. Whilst for the Second Law heat engine cycles the maximum power that can be extracted is independent of layout, a particular combination of both is shown to be most advantageous in the case of a novel configuration of the irreversible thermoelectric assemblies. The heat exchanger/thermoelectric converter is made up of a coaxial assembly of many annular elements in series and a section in which heat is rejected to the incoming reactants is followed by a second section which discards unconverted heat to cold surroundings. It is shown that the efficiencies of such devices substantially exceed the maximum efficiencies of the best present day thermoelectric conversion systems and the theory suggests practical designs for small, combustion driven, power supplies.

## **1. Introduction**

Hydrocarbon fuels have a specific energy content some two orders of magnitude greater than that of any electrical storage device, but conversion to electrical power is problematic. The search for compact, light-weight, long-lasting alternatives for batteries is motivated by the need to power the ever-proliferating portable electronic devices, such as equipment for infantry troops, for weather stations and buoys in polar regions which, unattended over long periods, need to signal their readings intermittently to passing satellites, and many others. Fuel cells, converters based on miniaturised gas turbines, and other systems under intensive study, give rise to diverse practical difficulties. Thermoelectric devices are robust, durable and have no moving parts, but tend to be exceedingly inefficient. However, because of their inefficiency, a large proportion of the heat rejected at their cold junctions can be recycled. This suggests the prospect of associating them with the kind of counter flow heat exchanger that underlies heat recirculating combustion systems. The objective of this study is to establish theoretical limits to conversion efficiencies from combustors in which the reactants (or the combustion air alone) are preheated using heat recycled from beyond the flame zone, without mixing the two streams. As a first step, in this paper we establish these maxima without regard to practical limitations due to heat losses, finite rates of heat transfer and chemical reaction, etc.

## 2. The burner system

Combustion systems in which the reactants or the air alone are preheated using heat "borrowed" from the region downstream of the flame zone offer significant advantages as regards fuel conservation, efficiency and combustion intensity; they have sometimes been referred to in terms of their "excess enthalpies" or "super-adiabatic flame temperatures." A great variety of such devices has been described, all of which are based on a combustor located between the two limbs of a heat exchanger (for reviews see, *e.g.*, refs 1, 2).

Figure 1 shows in the simplest possible way the various temperature intervals between product and reactant limbs of the heat exchanger as a function of mixture composition, flow rate and calorific value, heat recirculation,  $R$ , and heat abstraction,  $W$ , (*e.g.*, by a converter) for a lean, premixed flame. For simplicity, the discussion that follows will be based on the heat exchange and burner scheme illustrated in Fig. 2. The temperatures,  $T$ , at strategic points are denoted by suffixes as follows:  $o$  = ambient,  $u$  = unburnt (just upstream of flame),  $b$  = burnt (just downstream of flame),  $f$  = final (at heat exchanger exit). For a particular specific heat capacity,  $c$ , and mass flow rate,  $M$ , both assumed constant, we can arrange the dimensions and geometry so as to give the specified temperature intervals. The chemical heat release rate is  $MfQ$  ( $Q$  = heat of combustion/mass of stoichiometric mixture,  $f$  = fraction of stoichiometric fuel concentration) and heat losses from the heavily insulated system are neglected. The mixture consists mostly of air (> 99.5% close to the flammability limit) and even  $T_b$  is too low for dissociation. In the absence of heat abstraction or losses (as shown in the first and second temperature profiles), heat recirculation does not affect the steady-state exit temperature but may result in a greatly elevated flame temperature and hence reaction rate in premixed systems, and thermodynamic efficiency in the case of a converter - subject only to the thermal limitations of the heat exchanger and of reactant pre-ignition.

The third temperature profile shows heat abstraction, in this particular case upstream of the high-temperature side of the heat exchanger. Clearly, the absolute maximum  $W$  allowed by energy conservation is  $MfQ$ , if a steady state is to be maintained. (As further discussed below, this maximal level of heat extraction would require an idealised heat exchanger, transferring heat across an infinitesimal temperature difference since, with  $W = MfQ$ , the outlet temperature of the cold side of the heat exchanger is equal to the inlet temperature of the hot side of the heat exchanger.)

The position, and thus the temperature range, where heat is abstracted is a variable - it may be more advantageous to arrange it to overlap or have it upstream or downstream of the high temperature side of heat exchanger. The same variability applies to heat rejection (not shown in Fig. 1) that would be associated with heat abstraction for a heat engine - *e.g.* a thermoelectric converter. The main objective of this paper is to determine the effect of the position, and thus temperature, of heat abstraction and heat rejection so as to optimise the overall thermal efficiency of the device.

### 3. Converter

Figure 3 shows a design of heat exchanger/thermoelectric converter we set out to parallel the heat flow geometry of Fig. 2. It consists of a coaxial assembly of a large number of flat annular "washers" made up of alternating n-type and p-type thermoelectric materials connected in series. They are joined alternately at their inner and outer peripheries, in the manner of compressed concertina bellows. Except at these hot and cold junctions, they are separated by insulating material, prior to being compressed axially. They are represented by the crenelated lines in Fig. 3. Power is extracted through leads at the ends of the assembly. The cold junctions constitute the inlet limb of the heat exchanger, so that the device acts as both a generator and as the heat exchanger of Fig. 2 - see Fig. 3 (ii). Alternatively, the cold side can be maintained at ambient temperature as shown in Fig. 3 (i).

### 4. Efficiencies

Since the efficiency of each element of the converter is a function of both the hot and cold temperatures ( $T_h$ ,  $T_c$ ) and the temperatures depend on the energy abstracted further upstream, we need to consider three kinds of efficiencies. If  $w$  is now the electrical power output and  $q$  the thermal input rate, the **basic efficiency** of each element,  $\eta = \delta w / \delta q$ . Since  $\delta q = -Mc \delta T_h$ ,  $w = -Mc \eta \delta T_h$ , and  $Mc(1-\eta) \delta T_c$  is rejected to the heat sink, which may be the reactant stream. Integrating  $\delta w$  over the resulting temperature range yields the **global efficiency**,  $\eta_g = (w/q)$ . The maximum value of  $q$  (the heat abstracted for the converter) is  $MfQ$  (the heat release due to combustion as shown in Fig. 1), so that integrating  $\delta w$  over appropriate temperature range gives the **effective system efficiency**,  $\eta_e = w/MfQ$ . It is obvious that the highest system efficiency will be obtained by maximising  $T_h$  by heat recirculation and minimising  $f$  by burning the least proportion of fuel - the former being limited by either the temperature limit of the materials or the heat transfer coefficients, the latter by flame stability limits. What is less immediately obvious is whether rejection of the unconverted heat to the cold surroundings or to the incoming reactants as part of the heat recirculation process will yield the higher system efficiency. This question is addressed in the following sections.

### 5. Second Law maxima

It will be useful to establish absolute theoretically maximum efficiencies first, as a benchmark for the less efficient irreversible thermoelectric converters. For each elemental Carnot cycle,

$$\eta = 1 - (T_c/T_h) \dots \dots (1)$$

The above integration to obtain the global efficiency,  $\eta_g$ , has been carried out in previous work [1, 3] both for the case of heat rejection to the ambient cold surroundings,  $T_o$ , as in figure 3(i) and for

the case of heat rejection to the incoming reactants, figure 3(ii). The results are, respectively,

$$\eta_g = 1 - [(T_o/(T_{h,u} - T_{h,l}))]^* \ln(T_{h,u}/T_{h,l}).....(2)$$

and

$$\eta_g = 1 - (T_{c,l}/T_{h,l}) = 1 - (T_{c,u}/T_{h,u}).....(3a)$$

The suffixes  $u$  and  $l$  stand for the upper and lower bounds of the temperature ranges. Note that

$$(T_{c,l}/T_{h,l}) = (T_{c,u}/T_{h,u}).....(3b)$$

We apply this first to an idealised system - that illustrated in the third part figure 1 - which would intuitively be expected to yield an absolute efficiency maximum: a hypothetically perfect heat exchanger that operates on an infinitesimal temperature difference, surmounted by a converter which uses all the heat of combustion at the maximum temperature and rejects heat to the ambient cold surroundings, as shown in figure 3 (i). For this idealized maximum efficiency case

$$\eta_g = 1 - [(T_o/(T_b - T_u))]^* \ln(T_b/T_u) \quad (4),$$

Also  $\eta_g = \eta_e$  in this case

It is instructive to estimate some numerical values of this maximum-efficiency generator.  $T_b$  is limited by both flame stability and the tolerances of the working materials. It has been known for a long time [15] that, to a sufficient approximation, the lean limits of flammability vary with preheat in such a way as to keep  $T_b$  constant - say at 1500K. The limiting value varies somewhat for different fuels (and greatly with the use of catalysts, see [14]), but 1500K is reasonable for methane or natural gas [4 - 6] Taking room temperature,  $T_o$ , as 293K, the efficiency is

$$\eta_g = 1 - [(293/(1500 - T_u))]^* \ln(1500/T_u) = 1 - [(293/(1500 - T_u))]^* \ln[1500/(293 + R/Mc)] = \eta_e..(5)$$

This is shown as the upper curve of Fig.4, plotted against the preheat temperature rise,  $(T_u - T_o) = R/Mc$ . Good, well insulated, heat re-circulating burners achieve  $T_u = 1200K$  (see ref. 7) corresponding to a combustion heat release of only 300K needed to reach the 1500K level to sustain reaction. We shall henceforth use these temperatures as a standard for good heat re-circulating burners and refer to them as **SBT**. Thus the maximum theoretical efficiency for SBT is **0.782**.

In the absence of heat recirculation, combustion would have to raise the incoming fuel-air mixture from 293K to 1500K and the efficiency would drop to 0.604. Thus the increase in the maximum theoretically possible efficiency due to heat recirculation preheating by 907K is 29.5%.

We now compare this with case (ii) of figure 3. This is essentially represented by the second sketch of figure 1, except that a fraction of the heat recirculated,  $R$ , is extracted as electrical power. Here the global efficiency for maximum energy recycle

$$\eta_g = 1 - (T_o / T_f) = 1 - (T_u / T_b) \dots\dots(6a)$$

which is clearly much less because of the raised rejection temperatures, though it operates on a potentially much greater heat input. Using the same numerical values,

$$\eta_g = 1 - (293 / T_f) = 1 - (293 + R/Mc) / T_b \dots\dots(6b)$$

The corresponding global efficiency for SBT is 0.2. Note that the exit temperature,  $T_f$  is fixed in this case (= 366.25K for SBT) by the requirement to reject the unconverted heat so as to maintain a steady state. The global efficiency here works not on  $fQ/c$  but on  $R/Mc$  (= 1133.75 for SBT), yielding a power output  $W = \eta_g * (R/Mc)$  and a system efficiency,

$$\eta_e = \eta_g * (R/Mc) / (fQ/c) \dots\dots(7)$$

which yields  $\eta_e = 0.756$  for SBT. The system efficiency for case (ii) of figure 3, plotted against the preheat temperature rise, is shown as the middle curve in figure 4. It is always less than that for case (i) though it approaches it at large preheats and (ii) is less implausible practically, in that it does not require a hypothetical heat exchanger presumed to work on an infinitesimal temperature difference.

There is, crucially, an interesting third case, which is illustrated in figure 3 (iii). Although the exit temperature from the heat recirculating stage,  $T_f$ , is fixed in case (ii), there is no reason why we cannot discard the unconverted heat through another section of the converter, so long as its cold side is at ambient temperature,  $T_o$ , and not part of the heat recycle. In practice, this only requires the converter to protrude beyond the entry point of the heat exchanger section, as shown in figure 3(iii) and making it long enough to cool the product gases to near room temperature,  $T_o$ . The governing equation for this external second stage is the same as for 4 (i) - i.e. equation (4), so that the global efficiency for this part of the converter is

$$\eta_{g2} = 1 - [T_o / (T_f - T_o)] * [\ln(T_f / T_o)] \dots(8a)$$

which is 0.1074 for SBT. Thus the power output from this external section is

$$(T_f - T_o) * \eta_{g2} = (T_f - T_o) * [1 - T_o / (T_f - T_o)] * [\ln(T_f / T_o)] \dots(8b)$$

which is 7.867 for SBT. To calculate the system efficiency for case (iii), we sum the power outputs of the two stages

$$\eta_e = [\eta_{g1} * (R/Mc) + \eta_{g2} * (T_f - T_o)] / (fQ/c) \dots(8b)$$

or **0.782** for SBT. This is precisely the same as the system efficiency for case (i). Appendix 1 provides a formal proof that such is always the case **for Carnot cycles**. It should not be surprising that the maximum power that can be extracted according to the 2nd Law from a series of reversible engines with fixed maximum temperature and fixed ultimate heat rejection temperature must be the same. Thus the upper curve in Fig. 4 also represents the system efficiency for case (iii) of Fig. 3, whilst the lowest curve shows the contribution of its external stage - the importance of which decreases with increasing preheat temperature. In practice, the much smaller efficiencies of

real converters imply higher values of  $T_f$  and hence an increasing importance for the external stage in system (iii) of Fig. 3. In the next section we show that this system emerges as a generally advantageous configuration for real cycles.

### 6. Thermoelectric (irreversible) converters

We now apply precisely the same analysis to assemblies of irreversible engines such as semiconductor thermoelectric devices. The maximum efficiency of a thermoelectric device for given temperatures  $T_h$  and  $T_c$  is conventionally expressed [8 - 12] as

$$\eta = \frac{T_h - T_c}{T_h} \frac{\sqrt{1 + ZT_a} - 1}{\sqrt{1 + ZT_a} + T_c/T_h} \dots\dots\dots(10a)$$

where  $T_a = (T_h + T_c)/2$ , and  $Z (= \alpha^2\sigma/\lambda)$ , the “thermoelectric figure-of-merit”, is a measure of the effectiveness of the thermoelectric materials for energy conversion. Here  $\alpha$  = Seebeck coefficient,  $\sigma$  = electrical conductivity and  $\lambda$  = thermal conductivity. ( $Z^*T_a$  is sometimes referred to as the “dimensionless figure of merit”.) Since our objective is to calculate maximum attainable efficiencies and since we have the freedom to vary the thermoelectric materials (including segmented configurations) along the concertina - like structure to obtain optimum efficiency for different temperature ranges, we put  $ZT \approx 1$  as a typical maximum value for known thermoelectric materials. Thus

$$\eta = (T_h - T_c)/(3.44T_h + 2.44T_c) \dots\dots\dots(10b)$$

Using this as the basic efficiency of each element, we integrate  $\delta w$  the over appropriate temperature range, to obtain the global efficiency,  $\eta_g$ , following the same procedure as before for Carnot cycles in Section 5. For case (i) of Fig. 3, the global efficiency, which is also the system efficiency, is given by

$$\eta_g = [1/(T_{h,u} - T_{h,l})] \int_{T_{h,l}}^{T_{h,u}} [(T_h - T_c)/(3.44 T_h + 2.44T_c)] dT_h \dots\dots\dots(11a)$$

or in terms of the nomenclature of Fig. 1, and by analogy with equation (4),

$$\eta_g = [1/(T_b - T_u)] \int_{T_u}^{T_b} [(T_h - T_o)/(3.44 T_h + 2.44T_o)] dT_h = \eta_e \dots\dots\dots(11b)$$

where again  $T_o = 293K$  and  $T_b = 1500K$ . Hence,

$$\eta_g = [1/(1500 - T_u)] \int_{T_u}^{1500} [(T_h - 293)/(3.44 T_h + 715)] dT_h = \eta_e \dots\dots\dots(11c)$$

This is shown as the case (i) curve in figure 5 – plotted as before against the preheat temperature increment ( $T_u - T_o$ ). Again, applying this to SBT ( $T_u = 1200\text{K}$  and thus a preheat temperature increment of  $907\text{K}$ ) we obtain a system efficiency,  $\eta_e = \mathbf{0.197}$ .

Equation (11) also governs case (ii) of Fig. 3, except that, as with the reversible Carnot case,  $T_c$  is determined from the solution of  $\delta T_c = -(1 - \eta)\delta T_h$ . For the thermoelectric converter  $\eta$  is given by Eq. (10b) and thus

$$\begin{aligned}\delta T_c &= -[1 - (T_h - T_c)/(3.44 T_h + 2.44 T_c)]\delta T_h \\ &= -(2.44 T_h + 3.44 T_c)/(3.44 T_h + 2.44 T_c)]\delta T_h \dots (12)\end{aligned}$$

It is convenient to solve the relationship between  $T_c$  and  $T_h$  numerically. In the range of interest, it turns out to be almost linear and is well represented by

$$T_h = 233.9 + 1.0585 T_c \text{ and thus } T_c = 0.945 T_h - 221,$$

so that, for  $T_o = T_c = 293\text{K}$ , the temperature at which the products exit the heat exchanger,  $T_h = T_f = 544\text{K}$ .

Now,  $\eta_g$  is given by equation (11). Substituting for the variable  $T_c$  from above,

$$\eta_g = [1/(T_{h,u} - T_{h,l})] \int_{T_{h,l}}^{T_{h,u}} [(T_h - \{0.945 T_h - 221\})/(3.44 T_h + 2.44\{0.945 T_h - 221\})] dT_h \dots (13a)$$

for our system. Applying this to our SBT,

$$\begin{aligned}\eta_g &= [1/(1500 - 544)] \int_{544}^{1500} [(0.055 T_h + 221)/(5.75 T_h - 539)] dT_h \quad (13b) \\ &= 0.0564\end{aligned}$$

This low value illustrates how much  $\eta_g$  is degraded by allowing the heat sink temperature to rise. However, this efficiency now operates on the much larger heat input of  $Mc(T_b - T_f)$ , so that the system efficiency for our SBT,

$$\begin{aligned}\eta_e &= [1/(1500 - 1200)] \int_{544}^{1500} [(0.055 T_h + 221)/(5.75 T_h - 539)] dT_h \quad (14) \\ &= \mathbf{0.18}\end{aligned}$$



- a much more respectable value. Moreover, the larger  $T_f$ , the larger the residual heat input to the external second stage, when we convert case (ii) into case (iii) of figure 3.

The equation for the second stage of (iii) is again the same as for (i) - i.e. equation (11) – but with a temperature range  $T_f$  to  $T_0$ . The global efficiency becomes

$$\eta_{g2} = [1/(T_f - T_0)] \int_{T_0}^{T_f} [(T_h - T_0)/(3.44 T_h + 2.44T_0)] dT_h \dots \dots \dots (15a)$$

and, for our to SBT

$$\eta_{g2} = [1/(544 - 293)] \int_{293}^{T_f} [(T_h - 293)/(3.44 T_h + 715)] dT_h \dots \dots \dots (15b)$$

so that the power generated by this second section is

$$W_2 = \int_{293}^{T_f} [(T_h - T_0)/(3.44 T_h + 2.44T_0)] dT_h \dots \dots \dots (15c)$$

$$= 13.82$$

The power generated by the first section follows directly from equation (14) as 54. Thus the system efficiency of the two stages of system 4(iii) combined is

$$= \mathbf{0.226}$$

Unlike in the case of Carnot cycles, the system efficiency of system (iii) here exceeds that of system (i) (and, of course, that of system ii) as well as being feasible in practice, since it does not require heat transfer across an infinitesimal temperature difference. Similar conclusions are obtained for other preheat and flame temperatures.

Here again, a comparison with the efficiency in the absence of heat recirculation (with its requirement for an approximately 4 times higher fuel concentration to attain stable burning) is instructive. The efficiency (see Eq. 11a) would be

$$\eta_g = [1/(1500 - 293)] \int_{293}^{1500} [(T_h - 293)/(3.44 T_h + 715)] dT_h = \eta_e \dots \dots \dots (11d)$$

$$= 0.143$$

Thus the increase in the system efficiency due to this amount of heat recirculation is some 58%!

Since some thermoelectric materials are becoming available for which  $ZT_a > 1$ , it is pertinent to

consider how the advantage of system (iii) over those of (i) and (ii) depends on the thermoelectric figure-of-merit . Figure 6 shows that, for all practical values of  $ZT_a$ , case (i) is superior to case (ii) and the benefit of case (iii) over case (i) increases with  $ZT_a$ . Now, as  $ZT_a \rightarrow \infty$ , the thermoelectric efficiency reverts to that of the Carnot cycle - see equation (10a) - and the curves of figure 6 indeed converge at very large  $ZT_a$ . The maximum in the difference occurs at values of  $ZT_a$  too large to be of practical interest.

## 7. Conclusions

The performance of thermoelectric converters that, in rejecting unconverted heat, act as heat exchangers in heat recirculating burners, has been considered theoretically. The question of whether higher system efficiencies are realisable by rejection of the unconverted heat to the cold surroundings or to the incoming reactants as part of the recycle (compare figures 3 i and ii) was resolved, generally in favour of the former. However, a particular combination of the two - see figure 3(iii) - in which rejection of the unconverted heat to the incoming reactants is followed by a second section of the converter which discards unconverted heat to cold surroundings, is shown to be superior to either, on the grounds both of efficiency and practicability. We emphasize that all the system efficiencies that follow are theoretical upper limits to what may be attainable.

Although some heat recirculating furnaces now operate at much higher temperatures (e.g. 13) we have used as our standard model a preheat of 1200K and confined our maximum flame temperature to 1500K – close to the limit of what constitutes a flammable mixture - because of limitations imposed by the tolerances of thermoelectric materials. Such magnitudes have previously been achieved in near – limit combustion in practice (e.g. 1).

The absolute maximum system efficiency permitted by the 2nd Law for the assumed preheat and maximum temperatures is shown to be 78.2% and is the same for cases (i) and (iii). This represents an increase over the theoretical maximum efficiency in the absence of heat recirculation of some 29.5%.

The absolute maximum system efficiency for idealised thermoelectric devices which double as heat exchangers is greatest for case (iii) at 22.6 % - which is almost 29% of the maximum

permitted by the 2nd Law. It is also an improvement of some 58% over the case without heat recirculation.

Although the above treatment is purely theoretical, the greater practicability of system (iii) is vital. In burning fuel - lean mixtures, the struggle against heat losses assumes major importance. In lengthening a heat exchanger to achieve a desired exit temperature, heat losses increase proportionately. Such losses are especially important for small-scale generators because of their high surface area to volume ratios. This is particularly damaging in case (i) - quite apart from having to hypothesise an idealised heat exchanger which operates on an infinitesimal temperature difference. By contrast, heat losses are substantially diminished in the first stage of case (iii), because they occur from the cold limb of the heat exchanger while, in its second stage, they are an essential part of the generating process.

### References

1. F . J . Weinberg " Advanced combustion methods " Ch. 3 . "Combustion in heat - recirculating burners." Academic Press, London and New York, (1986).
2. Weinberg Felix , Combustion Science and Technology, 121:3 (1996).
3. Hardesty D.R. and. Weinberg F.J, Combustion Science & Technology, 12: 153 (1976)
4. Lloyd, S.A. and Weinberg, F.J. . Nature 257: 367.(1975)
5. A.R., Lloyd, S.A. and Weinberg, F.J. . Proc. Roy. Soc. A 360: 97 (1978).
6. Khoshnoodi, M. and Weinberg, F.J. . Combustion & Flame, 33:11 (1978).
7. Lloyd, S.A. and Weinberg, F.J. . Nature, 251:47 (1974).
8. Ioffe,A F Semiconductor Thermoelements and Thermoelectric cooling, Infosearch, London, (1957)
9. Rowe, D M and Bhardari C M, Modern Thermoelectrics, Holt, Rinehart and Winston, (1983)
10. Goldsmid, J H, Electronic Refrigeration, Pion, London, (1986)
11. Rowe D M, "CRC Handbook of Thermoelectrics", CRC press, London, (1996)
12. Min G., Rowe D M and Zhang J S, "Thermoelectric Energy Conversion and Applications", Weaponry Industries Publishing Co., Beijing, (1996)
13. Katsuki, M. and Hasegawa, T. Proc. 27th (Int.) Symposium on Combustion, The Combustion Institute, Pittsburgh, 1998, p. 3135.
14. Sitzki, L., Borer, K., Wussow, S., Schuster, E., Ronney, P. D. and Cohen, A., "Combustion in Microscale Heat-Recirculating Burners," Paper No. 2001-1087, 39th AIAA Aerospace Sciences Meeting, Reno, NV, January 8-11, 2001.
15. White, A. G. (1925), j. Chem. Soc., 127: 672.

## Appendix 1

Consider the power generated in each of the cases:

Case (i):  $W = T_b - T_u - [T_o \ln(T_b/T_u)]$

Case (iii) 2nd stage:  $W = T_f - T_o - [T_o \ln(T_f/T_o)]$

Case (iii) 1st stage:  $W = T_b - T_f - (T_b - T_f)T_o/T_f$

where  $T_b/T_f = T_u/T_o$  i.e.  $T_f = T_o T_b/T_u$

Case(iii) sum stages:

$$\begin{aligned} \sum W &= T_o T_b/T_u - T_o - [T_o \ln(T_b/T_u)] + T_b - T_o T_b/T_u - (T_b - T_o T_b/T_u) T_u/T_b \\ &= T_b - T_u - [T_o \ln(T_b/T_u)] \quad \text{QED.} \end{aligned}$$

Thus the maximum system efficiency for any arrangement of stages, in terms of the preheat temperature and  $(fQ/c)$  temperature rise across the flame is

$$\eta_{e,max} = 1 - (cT_o/fQ) \ln[(T_u + fQ/c)/T_u]$$

### **Figure Captions**

Figure 1 - Basic heat balance showing temperature intervals for premixed adiabatic systems.

Figure 2 - Schematic of burner system

Figure 3. Schematic of three heat exchanger - converter configurations.

Figure 4. Carnot system efficiencies vs. preheat temperature.

Figure 5. Thermoelectric system efficiencies vs. preheat temperature

Figure 6 Effect of figure of merit ( $ZT_a$ ) on system efficiency for the three cases of figure 3

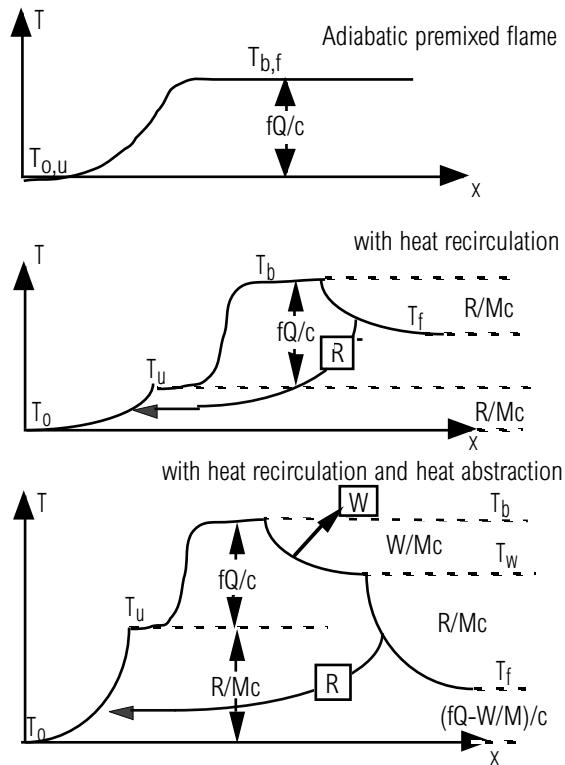


Figure 1 - Basic heat balance showing temperature intervals for premixed adiabatic systems.

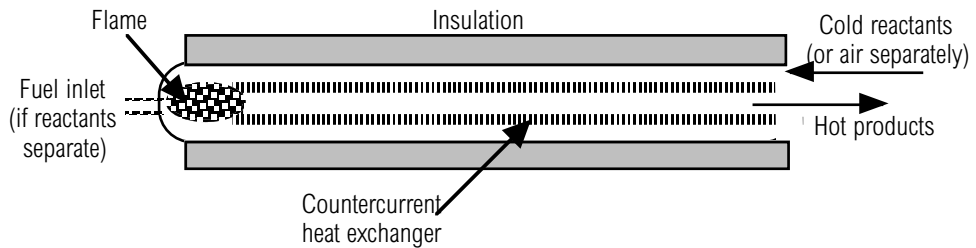


Figure 2 - Schematic of burner system

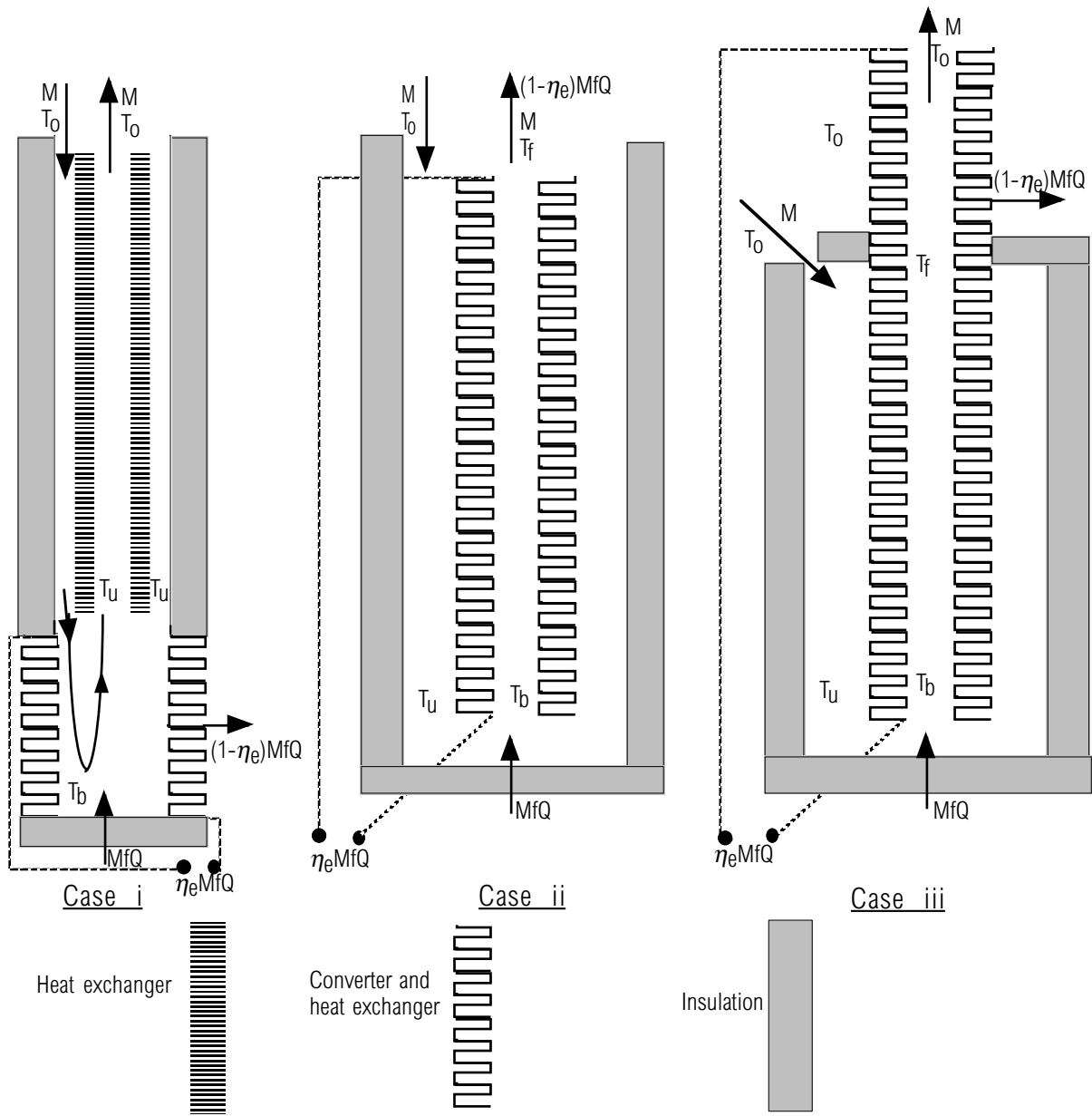


Figure 3. Schematic of three heat exchanger - converter configurations.

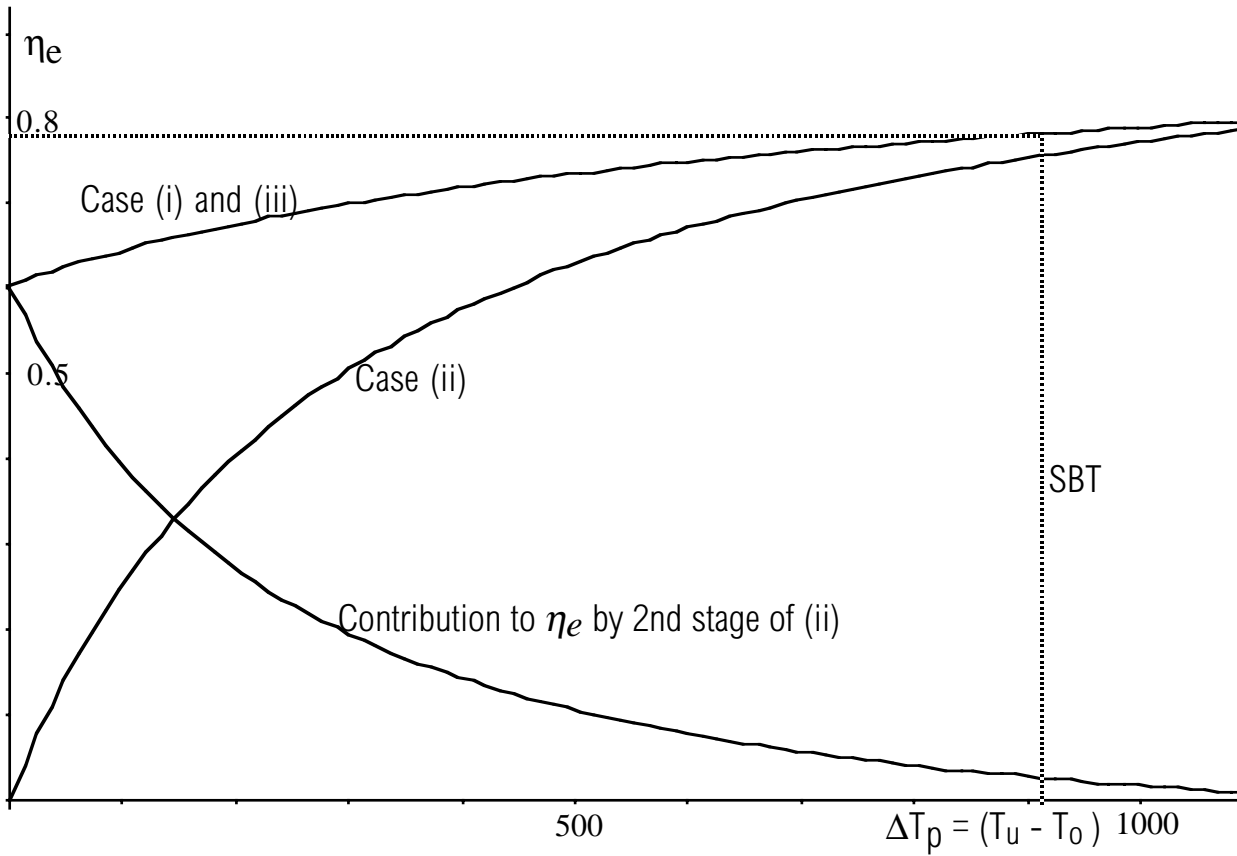


Figure 4. Carnot system efficiencies vs. preheat temperature.

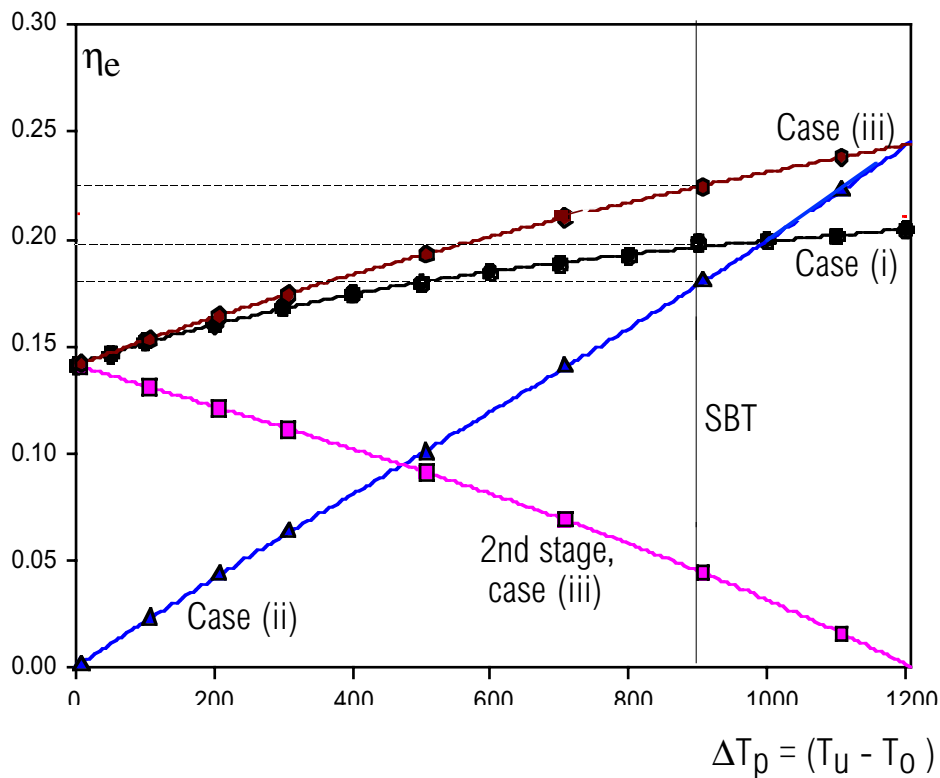


Figure 5. Thermoelectric system efficiencies vs. preheat temperature



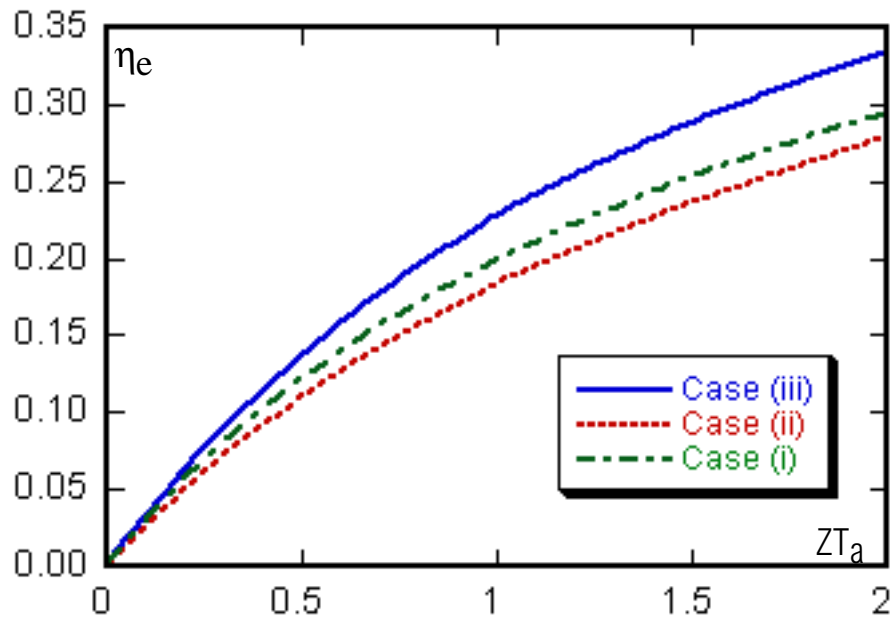


Figure 6 Effect of figure of merit ( $ZT_a$ ) on system efficiency for the three cases of figure 3